Segmentation of Optical Coherence Tomography Images for Analysis of Fluid Related Abnormalities

Venkatraman K[1] and Sumathi M[1]

[1]School of Electronics and Communication Engineering, Sathyabama Institute of Science and Technology, Chennai, India.

(Received: Jul 2018 Revised: Oct 2018 Accepted: Dec 2018)

Corresponding Author
Venkatraman K. E-mail: *venkat.biomed@gmail.com*

ABSTRACT

Introduction and Aim: Optical coherence tomography is a prominent ophthalmic diagnostic tool that serves a noninvasive, depth-resolved imaging modality. Hence, Automation in the analysis of these images is emerging as an important screening tool for early detection of eye diseases like Cystoid macular edema (CME), Symptomatic exudates-associated derangements (SEAD) which serve prior stages of Vision loss.

Materials and Methods: The features of the Retinal Layers could be evaluated for this purpose, which shall further be used in the identification and classification of the fluid related disorders using a Classifier. This can also be used to determine the extent to which the retina is affected, and hence, proper therapy could be inducted, thereby avoiding vision loss. As a prior stage to these procedures, the evaluation of two different techniques of segmentation, Sobel filter and watershed algorithm are discussed in the various sections.

Results: The methodologies were implemented with 35 different images acquired from Zeiss OCT Device using MATLAB R2015a. Results show that both the techniques are equally efficient and could be used as a robust and precise system to study and analyse the Optical coherence tomography Images.

Conclusion: When compared with the other prevailing techniques, the developed systems have comparatively been evaluated for a larger set of input data, thereby classifying a wider range of diseases.

Key Words: Edema, Fundus Imaging, Retinal disorders, Segmentation

INTRODUCTION

Diabetes is the major cause of blindness in the world; it is because of various disorders like Cystoid macular edema and Symptomatic exudates-associated derangements, which are caused due to elevated levels of blood glucose (1). This is mainly because of the excessive accumulation of fluids in the retinal layer. It activates the interior layer of eyes to convert the event light falls into neural segments signals for transmission to the brain. The damages in these layers may result in several abnormalities that include vision loss. In other words, automation in the diagnosis of fluid volume is expected to contribute significantly to the earlier detection and treatment of such disorders. These fluid related abnormalities are screened using an ophthalmic device, Optical Coherence Tomography (2,3). OCT is used to measure the reflections of the internal structures of the biological tissues. It serves as a vital tool in diagnosing several diseases, including Age-related macular degeneration (AMD), glaucoma, retinopathy, and CME.

Existing works in the OCT Image analysis focused on the segmentation of Intraretinal layers (4), segmentation of the fluid-filled regions and the optical disc. The advantage of using the OCT Image instead of Fundus photographs tools is the highly sensitive micron-scale resolution images (5). B mode and OCT ultrasound are more or less similar, except low coherent source is used. Optical Reflections of the internal structures are measured cross-sectionally in the OCT. There is useful information on the time of flight delay obtained from the coherence property of the reflected light (6). This delay is used to determine the longitudinal location of the reflection areas. Multiple longitudinal scans can be performed by the OCT System in a series of lateral locations by providing a two-dimensional mapping of the reflection areas in the sample. The rate of acquisition is enhanced by the continuous longitudinal motion scanning and making the two-dimensional imaging possibility occurred. Unlike Magnetic Resonance Imaging or X-Ray Computed Tomography, the reconstruction of OCT Images implements lesser computations. Measurement of the intraocular pressure frequently failed to analyze the progress of glaucoma. Abnormalities like loss of visual field and cupping of Optical Nerve Head (ONH) are clinically diagnosed only after 50% of Nerve fiber loss (7). Because of the cylindrical nature of the nerve fibers, the incident angle of light determines the backscattered signal from Retinal Nerve Fiber Layer (RNFL) (8,9). This accounts for the RNFL Signal attenuation, it is observed at the margin of the optic disc, where the nerve fibers descend into optic nerve (10). It gives an effective automated tool for the analysis of OCT images and provides earlier detection of these severe disorders and helps in identifying the problem of vision loss. For developing an efficient tool for diagnosis, it is essential to adopt a proper technique for segmentation, failing to which, the entire system provides the poor statement (11). And the pre-therapeutic and post-therapeutic could also be analyzed by the proper segmentation tool — the disorders caused in the abnormal fluid levels of the retina as shown in fig.1.

Figure 1: Retinal disorders CME, CNVM, MH, and ERM

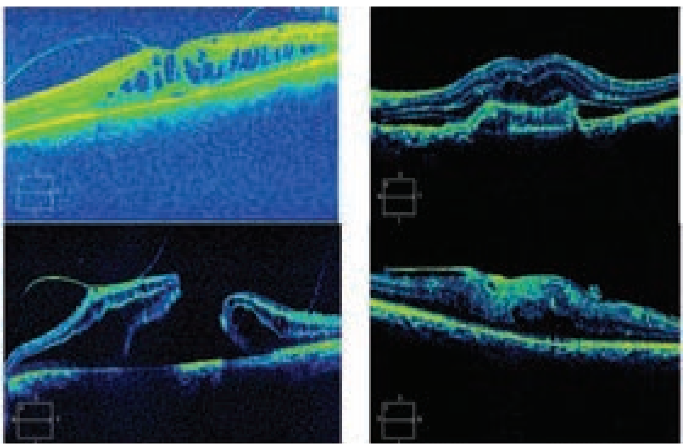

The experiment of this research delivers the segmentation of the retinal fluid volume for analysis of the severity of the abnormality. Further, these techniques can be used in the analysis of postoperative and post medicative effects in the patients. Various related works are discussed, further to which the results of the segmentation techniques are discussed. In this research, the segmentation is performed with a basic edge detection algorithm, and a watershed segmentation technique (12). The results are compared, and the conclusions are drawn based on the same.

Related Works

According to the survey in OCT, the process of segmentation is of higher importance because it also helps in the statistical analysis of retinal misalignments. Nevertheless, it also serves as a vital tool towards the evaluation of therapeutic efficiencies. Below discussed are various works related to the proposed work.

The anisotropic diffusion filter followed by GVF based snake algorithm for segmentation was proposed by Perona and Malik, based on multiscale edge detection, and this technique was efficient when compared to the Gaussian filtering (13). The edge preservation was then analyzed by a correlation parameter, χ, which was expected to be close to unity for the optimal effect of edge preservation. After noise removal and the lesions isolation, the quantitative analysis of the surface area, and the volume were performed, and segmentation was done by the snake algorithm. A Gradient Vector Flow (GVF) based snake was used in the preprocessed OCT images to obtain accurate shape in regions filled with fluid, associated with AMD. The optimum values of the GVF Snake contour fitting the lesion boundary in the images were also identified. The performance of the snake model (SM) for peripheral, central, and multiple regions with fluid in the OCT images was analyzed. The overall system efficiency was based on the noise filtering on which the snake converged with the boundary of lesions. And the initialization of the snake had to be manually analyzed; it required expertise towards initializing and guiding the snake for proper convergence.

Gwenole Quellec *et al*. determined the footprints of fluid-filled regions, called Symptomatic Exudate Associated Derangements (SEADs). The automated SEAD detection method was implemented with interactive segmentation. It remained a complex approach, as it involves three-dimensional image analyses. The system included intraretinal layer segmentation, textural features extraction from the segmented layers, and k-NN Classifier. By using this data binary, SEAD footprint images were obtained using a probability map followed by a thresholding technique. In addition to existing techniques of Intraretinal layer segmentation (10) fast multi-scale 3D graph search method was introduced, to detect the three additional retinal surfaces from 3D OCT scans centered at Optic Nerve Head (ONH). Ten Intraretinal layers were automatically segmented by a multi-scale three-dimensional graph search technique (8). Flattening of the macula in the image was achieved by using the last retinal surface as a reference plane, after which the three-dimensional textural feature extractions were done (14). Features were calculated in the flattened layer sub volumes. The detection of SEAD footprint under various circumstances was analyzed. The methodology proposed was interactive yet tedious and time-consuming when compared to the techniques existed.

Xinjian Chen *et al*. proposed a system for automated segmentation of SEAD Volumes of AMD Patients (15). The algorithm was divided into two parts, retinal layer segmentation, and the probability constrained combined graph search graph cut method. The segmentation of SEADs remains a tough task due to low SNR and Shape Variability; the algorithm implemented an automated volume segmentation in three dimensional OCT Images (16). The automated segmentation tool failed to segment up to 30% of the analysed scans. A surface region graph-based approach (17,18) was proposed for the segmentation of multiple regions and multiple surfaces simultaneously.

Eleven Layer Segmentation of the retina was initially performed for initializing the process of segmentation by identifying the voxels with fluid (1). Various positional, textural, and structural features of the voxels were calculated, based on which voxels were classified. A binary image was hence obtained using the positive and negative voxels in the dataset. The classification was based on the k-NN Classifiers (19). After the training phase, the segmentation was tested with the unknown sample. The sub graphs were generated in relation to the previous works. The validation process was so efficient that it included cross verification by the manual segmentation performed by the retinal specialist using the software described in. The statistical relativity of the manual and automated segmentation was analyzed by linear regression analysis and Bland-Altman plots. The algorithm seems to be reliable and fully automated, and the performance was based on the results of initialization. If the probability Constraints were false, then the entire result was a failure.

Gray.R.Wilkins *et al*., inferred that the Macular thickness measurement could be erroneous in the presence of subretinal fluid (14). The system was constructed to identify the regions of cystoid fluids within the 3D stack, using the elimination technique for the False Positive (FP) from the Region of Interest. The algorithm included noise removal, gray level conversion, and retinal layer segmentation, bilateral filtering, thresholding, tracing of the boundaries and the FP rejection. The design was user-friendly which executed a single function whose only input was the stack image. By the efficiency of sensitivity and specificity of 91% and 97% respectively, the system required lesser computation time; the blood vessels were also rejected during the process of FP rejection. The algorithm analyzed for a small database. Also, the system ability to differentiate the cyst and Intraretinal layers were not evaluated, which could have been taken into consideration.

Chuang Wang *et al*. developed the automatic choroidal layer Segmentation using Markov Random Field Method. The algorithm was based on the change in the thickness of the choroidal layer, which was related to numerous retinal disorders. Preprocessing used anisotropic diffusion filtering to remove the artifacts. The distance regularization and edge constraint terms were embedded into the level set method to avoid the irregular and small regions and hold information about the boundary between the choroid and sclera (19). The algorithm correlated the single-pixel likelihood function with neighborhood information to compensate for the inhomogeneous texture. The effectiveness was evaluated by comparing against other segmentation methods on a dataset. The proposed system was entirely suitable for choroidal abnormalities.

Jingyun Guo *et al*. focused on Branch Retinal Artery Occlusion (BRAO) in OCT images. Proposed was the first automatic 3D BRAO segmentation framework. The developed system classified the image as acute, chronic, and normal using the AdaBoost Classifier. Various local structural, intensity, textural features were used for this process of classification. A thickness model was built to segment BRAO in the chronic phase. While for segmenting BRAO in the acute phase, a two-step segmentation strategy was performed: rough initialization and refine segmentation (20). The proposed method was tested on the SD-OCT images of 35 patients, and results seemed to be accurate significantly.

Md Akter Hussain *et al.* designed the automated method to segment four layers of the retina from the SD-OCT images (21). The proposed algorithm located three reference layers, which then used the actual layers, which was analyzed by modeling and applying Dijkstra's shortest path algorithm. Though the results showed that the system was of higher accuracy and reliability, the evaluation was done with a considerably smaller database.

MATERIALS AND METHODS

It is evident from the literature survey based on OCT that a logical and effective tool for analysing the fluid filed abnormalities of the retina is the accurate fragmenting of the SD-OCT images that contain retinal layers with fluid-filled regions. The proposed methodology employs two different modes of segmentation (8). A simple Sobel edge detection is performed whereby thresholding is assessed. The algorithm that implements watershed segmentation is evaluated for various images.

The Sobel Edge detection filter, proposed by Irwin Sobel and Grey Feldman explained an idea of an "Isotropic 3x3 Image Gradient Operator". It creates an image emphasizing edges and performs a 2-D spatial gradient measurement on an image. It highlights the regions of high spatial frequency that is in accord to edges. The Sobel–Feldman operator is based on convolving the image with a compact, distinct, and integer-valued filter in the horizontal and vertical directions and hence is very basic and effortless in terms of ciphering. 3×3 kernels are used, where the original image is convolved to calculate the derivatives approximations – one for horizontal changes, and one for vertical, as shown in (1).

where, Gx and Gy are the vertical and horizontal matrices/ filter masks used for convolving the original image A.

$$\mathbf{G}_x = \begin{bmatrix} +1 & 0 & -1 \\ +2 & 0 & -2 \\ +1 & 0 & -1 \end{bmatrix} * \mathbf{A} \quad \text{and} \quad \mathbf{G}_y = \begin{bmatrix} +1 & +2 & +1 \\ 0 & 0 & 0 \\ -1 & -2 & -1 \end{bmatrix} * \mathbf{A} \qquad (1)$$

The x-coordinate is described as increasing in the "right"-direction, and the y-coordinate is described as increasing in the "down"-direction. At each point in the image, the resulting gradient approximations can be combined to give the gradient magnitude, using equation (2):

$$G=\sqrt{G_x^2+G_y^2} \qquad (2)$$

Further to the edge detection-based segmentation, the obtained edges are amplified by basic morphological operations, say skeletonization.

Watershed segmentation is another methodology used in segmentation, which treats the image as a topographic map in which the height of each point is represented by the brightness, and finds the lines that run along the top of ridges. The algorithm is defined using the following steps:

1. Each minimum is labeled with a distinct label wherein a set A is initialized with the labeled nodes.

2. Extricate from A a node x of minimal altitude F, that is to say, $F(x) = \min\{F(y)|y \in S\}$. Assign the label of x to each non-labeled node y adjacent to x, and insert y in A.

3. Step 2 is repeated until A is empty.

The SD-OCT images with abnormalities are assessed with these two methodologies of segmentation whereby the performance of the latter is examined with their outputs comparing each other.

RESULTS

Figure 2: Output of segmentation for various abnormal OCT Images

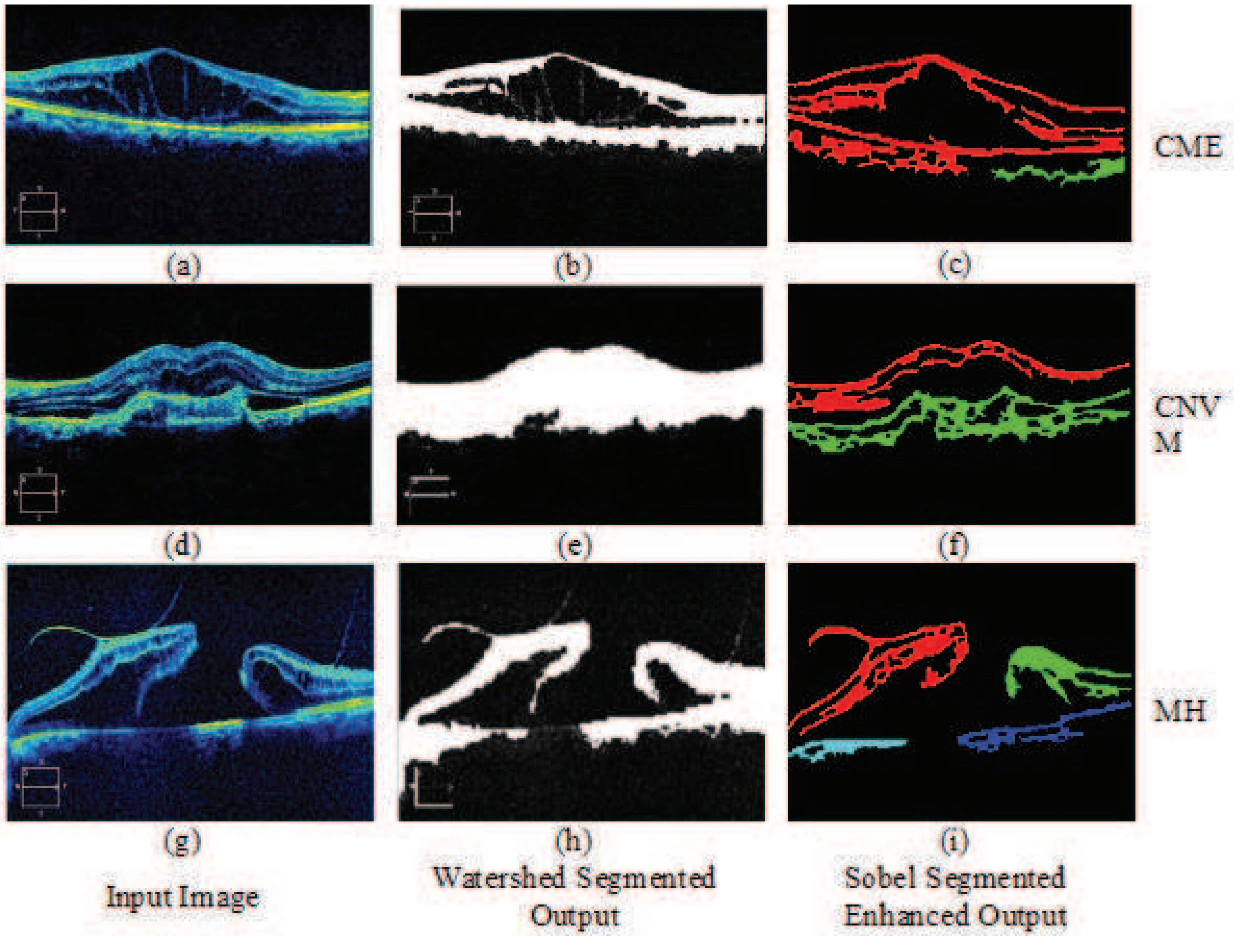

DISCUSSION

The SD-OCT images were obtained for various disorders including Cystoid Macular Edema (CME), Macular Hole (MH), Choroidal Neo Vascular Membrane (CNVM), and Normal images from 35 different patients obtained using ZEISS instrument. The overall processing was done using MATLAB. These images were further preprocessed for speckle removal. Median filters were used to remove the speckle noises from the input images (22-24). The preprocessed images were subjected to two different algorithms of segmentation to obtain the isolated region of fluid-filled abnormalities. The watershed algorithm is performed on the preprocessed image further to which it is enhanced by image dilation and erosion. On applying the Sobel algorithm of edge detection, post-processing is done with binary thresholding and morphological skeletonization (25). The outputs of the above process for the various abnormalities are shown in fig.2.

From the above output, it could be understood that both the techniques seem to be efficient towards segmenting the fluid-filled regions. On estimating various features and the fluid area, further analysis of these images could be done. The efficiency of therapy, response of the patient on therapy, variations in fluid volume can also be studied on a thorough analysis of these images. The above results could be utilized to develop a fully automated system which shall be designed to efficiently classify the above-stated abnormalities in the retinal layers, which are caused due to variations in the fluid levels in the intraretinal layers (11).

The evaluations were done qualitatively, which has ended up with 94.28%visually acceptable contours that were classified as good and fair extraction cases by an ophthalmologist. The mean difference between the extracted contours using the proposed algorithms is within the differences of 5 pixels. The same is the level of tolerance found between the automated method of segmentation and manual analysis of segmentation. It could be understood that both the segmentation techniques perform well with slight differences in the levels of accuracy.

CONCLUSION

The efficient segmentation methodology has been evaluated for a wider range of retinal disorders. The results prove that the detection of features of interest for efficient Diagnosis. Though the outputs seem to be promising, it could be understood that the qualitative analysis of the algorithm could be done with second opinions to improve the reliability of the results. As segmentation identifies the fluid-filled abnormal region, it is also essential to further quantitatively analyze the region to comment on the overall intensity of the abnormality and its progression in the retina.

REFERENCES

1. Wilkins, G.R., Houghton, O.M., and Oldenburg, A.L. Automated segmentation of intrarentinal cystoid fluid in optical coherence tomography. IEEE Trans. Biomed. Eng. 2013; 59(4): 1109-1114.
2. Chan., Lam, E.Y., and Srinivasan, V.J. Comparison of Kasai autocorrelation and maximum likelihood estimators for doppler optical coherence tomography. IEEE Trans. Med. Imaging. 2013; 32(6): 1033-1042.
3. Sun, S., Guo, Q., Lei, B., Gao, B.Z., and Dong, F. Image denoising algorithm based on contourlet transform for optical coherence tomography heart tube image. IET Image Process. 2013; 7(5): 442-450.
4. Kafieh, R., Rabbani, H., Hajizadeh, F., and Ommani, M. An accurate multimodal 3-D vessel segmentation method based on brightness variations on OCT layers and curvelet domain fundus image analysis. IEEE Trans. Biomed. Eng. 2013; 60(10): 2815-2823.
5. Avanaki, M.R.N., Cernat, R., Tadrous, P.J., Tatla, T., Podoleanu, A.G., and Ali, H.S. Spatial compounding algorithm for speckle reduction of dynamic focus OCT images. IEEE Photonics Technol. Lett. 2013; 25(15): 1439-1442.
6. Manojlovic, L.M. Novel Method for Optical Coherence Tomography Resolution Enhancement. IEEE J. Quantum Electron. 2011; 47(3): 340-347.
7. Miri, M.S., et al. Multimodal Segmentation of Optic Disc and Cup from SD-OCT and Color Fundus Photographs Using a Machine-Learning Graph-Based Approach. IEEE Trans. Med. Imaging. 2015; 34(9): 1854-1866.
8. Quellec., Lee, K., Dolejsi, M., Garvin, M.K., Abràmoff, M.D., and Sonka, M. Three-dimensional analysis of retinal layer texture: Identification of fluid-filled regions in SD-OCT of the macula. IEEE Trans. Med. Imaging. 2010; 29(6): 1321-1330.
9. Abràmoff, M.D., Garvin, M.K., and Sonka, M. Retinal Imaging and Image Analysis. IEEE Rev. Biomed. Eng. 2010; 3: 169-208.
10. Yazdanpanah., Hamarneh, G., Smith, B.R., and Sarunic, M.V. Segmentation of intra-retinal layers from optical coherence tomography images using an active contour approach. IEEE Trans Med Imaging. 2011; 30(2): 484-496.
11. Diener. Optical Coherence Tomography. Proseminar Inform. der Medizin. 2011; 1-16.
12. Acharjya, P.P., Sinha, A., Sarkar, S., Dey, S., and Ghosh, S. A new approach of watershed algorithm using Distance Transform applied to Image Segmentation. ISSN Int. J. Innov. Res. Comput. Commun. Eng. 2013; 1(2): 2320-9798.
13. Perona, P., and Malik, J. Scale-space and edge detection using anisotropic diffusion. IEEE Trans. Pattern Anal. Mach. Intell. 1990; 12(7): 629-639.
14. Giancardo, L., et al. Textureless macula swelling detection with multiple retinal fundus images. IEEE Trans. Biomed. Eng. 2011; 58(3 PART 2): 795-799.
15. Chen, X., Niemeijer, M., Zhang, L., Lee,

K., Abramoff, M.D., and Sonka, M. Three-dimensional segmentation of fluid-associated abnormalities in retinal OCT: Probability constrained graph-search-graph-cut. IEEE Trans. Med. Imaging. 2012; 31(8): 1521-1531.

16. Xu, J., Ishikawa, H., Wollstein, G., Kagemann, L., and Schuman, J.S. Alignment of 3-D optical coherence tomography scans to correct eye movement using a particle filtering. IEEE Trans. Med. Imaging. 2012; 31(7): 1337-1345.

17. Bogunovi, H., et al. Multi-Surface and Multi-Field Co-Segmentation of 3-D Retinal Optical Coherence Tomography. 2014; 33(12): 2242-2253.

18. Dufour, P.A., et al. Graph-based multi-surface segmentation of OCT data using trained hard and soft constraints. IEEE Trans. Med. Imaging. 2013; 32(3): 531-543.

19. Wang, C., Wang, Y.X., and Li, Y. Automatic choroidal layer segmentation using markov random field and level set method. IEEE J. Biomed. Heal. Informatics. 2017; 21(6): 1694-1702.

20. Guo, J., Shi, F., Zhu, W., Chen, H., and Chen, X. A framework for classification and segmentation of branch retinal artery occlusion in SD-OCT. Prog. Biomed. Opt. Imaging - Proc. SPIE. 2016; 9784(7): 3518-3527.

21. Hussain, M.A., et al. Automatic identification of pathology-distorted retinal layer boundaries using SD-OCT imaging. IEEE Trans. Biomed. Eng. 2017; 64(7): 1638-1649.

22. Niu, S., Chen, Q., de Sisternes, L., Rubin, D.L., Zhang, W., and Liu, Q. Automated retinal layers segmentation in SD-OCT images using dual-gradient and spatial correlation smoothness constraint. Comput. Biol. Med. 2015; 54: 116-128.

23. Edmund Hui-On, N.G., Kainam, T.W., and Jerry, C.L.L. Speckle-Noise Reduction Via Rotated Elliptical-Thresholding In an Homomorphic Complex-Wavelet Domain. Department of Electrical & Computer Engineering University of Waterloo Waterloo, Ontario. Comput. Eng. 2005; 585-588.

24. Hiremath, P.S., Akkasaligar, P.T., and Badiger, S. Speckle Noise Reduction in Medical Ultrasound Images. 2013; 7(1): 201-241.

25. Shi, F., et al. Automated 3-D retinal layer segmentation of macular optical coherence tomography images with serous pigment epithelial detachments. IEEE Trans. Med. Imaging. 2015; 34(2): 441-452.